ISSN 0016-7932, Geomagnetism and Aeronomy, 2014, Vol. 54, No. 5, pp. 645–654. © Pleiades Publishing, Ltd., 2014.
Original Russian Text © G.A. Mikhailova, O.V. Kapustina, S.E. Smirnov, 2014, published in Geomagnetizm i Aeronomiya, 2014, Vol. 54, No. 5, pp. 691–700.

Effects of Solar and Geomagnetic Activities in Variations of Power Spectra of Electrical and Meteorological Variables in the Near-Surface Atmosphere in Kamchatka during October 2003 Solar Events

G. A. Mikhailova[a], O. V. Kapustina[a], and S. E. Smirnov[b]

[a] *N. V. Pushkov Institute of Terrestrial Magnetism, Ionosphere, and Radiowave Propagation, Russian Academy of Sciences, Kaluzhskoe shosse 4, Troitsk, Moscow oblast', 142190 Russia*

[b] *Institute of Space Physics Research and Radiowave Propagation, Far East Division, Russian Academy of Sciences, ul. Mirnaya 7, Paratunka, Kamchatka, 684034 Russia*

e-mail: yumikh@izmiran.ru, sergey@ikir.kamchatka.ru

Received March 25, 2014

Abstract—We perform spectral analysis of records of meteorological (temperature, humidity, pressure of the atmosphere) and electrical (stress of quasi-static electric field and electric conductivity of air) variables observed simultaneously at the Paratunka observatory during the solar events of October 21–31, 2003. Also, we use simultaneous records of X-ray fluxes of solar radiation, galactic cosmic rays, and the horizontal component of the geomagnetic field. We show that the power spectra of the meteorological parameters under good weather conditions involve oscillations with a period of thermal tidal waves ($T \sim 12$ and 24 h) caused by the influx of thermal radiation of the Sun. During strong solar flares and geomagnetic storm of October 29–31 with a prevailing component of $T \sim 24$ h, their spectra involve an additional component of $T \sim 48$ h (the period of planetary-scale waves). With the development of solar and geomagnetic activities, the power spectra of atmospheric electric conductivity and electric field stress involve components of both thermal tidal and planetary-scale waves, which vary highly by intensity. In the power spectra of galactic cosmic rays accompanying the strong solar flares, components with $T \sim 48$ h were dominant with the appearance of additional (weaker by intensity) components with $T \sim 24$ h. The simultaneous amplification of components with $T \sim 48$ h in the power spectra of electric conductivity and electric field stress provides evidence of the fact that the lower troposphere is mainly ionized by galactic cosmic rays during strong solar flares and geomagnetic storms. The specified oscillation period with $T \sim 48$ h in their spectra, as well as in the spectra of X-ray radiation of the sun, is apparently caused by the dynamics of solar and geomagnetic activities with this time scale.

DOI: 10.1134/S0016793214050119

1. INTRODUCTION

Under good weather conditions within the model of a spherical capacitor formed by the Earth's surface and the lower boundary of the ionosphere, the conduction current in the global electric circuit (GEC) is determined by remote thunderstorm sources (the so-called global thunderstorm generator). Also, there are other additional global-scale generators in the ionosphere (in the dynamo region at $h \sim 100$–120 km), in the magnetosphere, in the upper atmosphere of polar latitudes (solar cosmic rays), and in the middle atmosphere ($h \sim 15$–25 km) (galactic cosmic rays).

The midlatitude surface atmosphere, as a GEC component, involves both global and local current sources: a convective generator and a seismic generator, which supplies the atmosphere with Rn, a radioactive gas. Cumulus clouds negatively charged in the lower part also should be attributed to local generators. Local generators are known to be strongly dependent on meteorological variables (temperature, pressure, humidity, and wind velocity), which in turn depend on solar activity. The ionospheric dynamo makes an insignificant contribution to atmospheric parameters (~5–10%) [Roble, 1985]. Under good weather conditions at midlatitudes in the near-surface atmosphere, the effect of solar cosmic rays and the magnetospheric generator should also be neglected. Even in polar latitudes, the contribution of the magnetospheric generator is ~±20% relative to the contribution of the thunderstorm generator [Roble, 1985].

With strong solar flares and geomagnetic storms as global processes, their influence is manifested primarily in variations in global current sourcing in the GEC. The results of the analysis of these effects at middle and high latitudes are given in many studies and are consistently reflected in the surveys [Roble, 1985; Rycroft et al., 2012] (including the solar event in August, 1972).

Similar solar events occurred in October 2003 and November 2004. A detailed analysis of temporal variations in the electric field stress and electric conductivity of air in the near-surface atmosphere of Kamchatka during these events was conducted by us earlier [Smirnov et al., 2013, 2014]. In these works, we have considered simultaneously observed variations in the local meteorological parameters (temperature, pressure, humidity, and wind speed), as well as solar and geomagnetic parameters (fluxes of X-ray radiation as an indicator of the level of solar activity, the fluxes of solar and galactic cosmic rays, *Dst*-variations, *Kp*-indices, and the horizontal component of the geomagnetic field). First used to study the effects of solar phenomena in atmospheric electricity of the near-surface atmosphere, this integrated approach made it possible to separate the contribution of global and local sources in temporal variations in electric conductivity of the atmosphere and the electric field stress.

The temporal variations in the aforementioned variables are naturally related to the atmospheric dynamics during this period. In this context, to detect more distinct cause-and-effect relationships between these variables, it made sense to investigate their frequency variations in a wide range of periods of atmospheric waves: thermal tidal waves (TTWs, $T = 4$–24 h) and planetary-scale waves (PSWs, $T > 24$ h). The first attempt in this direction was the study [Smirnov et al., 2013] for the solar events of November 2004. The present paper is a sequel to these studies for the solar events of October 2003.

2. ORIGINAL EXPERIMENTAL DATA

Figure 1 shows simultaneous observation data of the following variables from October 21 to 31, 2003.

Curve *1* describes the quasi-static electric field stress (the *Ez*-component) measured by a Pole-2 instrument with an accuracy of 0.3 V/m and a temporal resolution of 1 min, as well as the values of the *Dst*-index (nT) with a temporal resolution of 1 h (http://spidr.ngdc.noaa.gov/spidr).

Curves *2* and *3* describe electric conductivities of the atmosphere due to positive (λ_+) and negative (λ_-) ions, respectively, and measured by an Elektroprovodnost-2 instrument with a temporal resolution of 1 min.

Curves *4*–*8* describe the pressure (P, hPa), temperature ($T°$, C), humidity (V, %), precipitation, and wind speed (U, m/s), respectively, measured with a temporal resolution of 10 min at WS-2000 and WS-2300 digital stations. The resulting data are transmitted to the observatory over a radio channel at a frequency of 433 MHz. Curve *4* has an additional curve for the record of the horizontal component of the geomagnetic field (H, nT), measured by an FRG-601G ferroresonant magnetometer with an accuracy of 0.01 nT and a temporal resolution of 1 min.

Curves *1*–*8* reflect the results obtained from observations at the Paratunka observatory ($\varphi = 58.9°$ N; $\lambda = 158.25°$ E; $\Phi = 46.37°$; $L = 2.1$). Also, observational data on the state of cloudiness and precipitation at a local meteorological station were used. Unfortunately, the observatory provided no actinometric observational data.

Curve *7* describes three-hour values of the *Kp*-index.

Curve *9* describes the fluxes of galactic cosmic rays (N is the number of particles per min) measured by a neutron monitor with a temporal resolution of 1 min at the Stekolny observatory (Institute of Space Physics Research and Radiowave Propagation, Far East Division, Russian Academy of Sciences).

Curve *10* describes the series of solar flares measured in X-ray fluxes (W/m^2) by the GOES-12 satellite http://goes.ngdc.noaa.gov/data/avg).

In addition to this figure, the Table shows a more detailed history of these events described in depth by Veselovskii et al. [2004], and Fig. 2 shows a close-up view of the series of several of the most interesting fragments of records of electric conductivity and electric field stress as a function of time UT (the local noon and midnight at the observatory correspond to 0145 UT and 1055 UT, respectively). A detailed analysis of temporal variations in the records shown in Fig. 1 was performed in [Smirnov et al., 2013]. Below, the results of their spectral analysis are presented.

3. SPECTRAL PROCESSING

To estimate the spectral power density (hereafter, power spectrum), we used the classical method of periodograms. The choice of length T of the time window ($T = 2$ days) is explained by the duration of periods of anomalous bursts of solar (October 22–23, 26–27, 28–29, 29–30) and, accordingly, geomagnetic (October 24–25, 29–30, 30–31) activities. Next, we used the method of superposed epochs; the good weather days of October 21–22 preceding the emergence of a strong solar flare on October 23 were chosen as reference days for comparison. During this period, the conditions of good weather were really retained: we had a low wind speed with $U < 4$ m/s, no precipitation, high stratus clouds, quiet solar activity manifested in regular diurnal variations of temperature and humidity, relatively quiet geomagnetic activity ($Kp \sim 4$), and diurnal variations (typical for these conditions) in electric conductivity and the *Ez*-component of the field (Fig. 2a) [Smirnov, 2013]. Since the meteorological variables were digitized with a temporal resolution of $\Delta t = 10$ min, all of the data used for spectral processing and digitized with $\Delta t = 1$ min were reduced to a time step of $\Delta t = 10$ min. The calculated power spectra S of all of the variables under analysis are shown in Fig. 3 on a linear scale, with the exception of X rays, which vary in a very wide range (10^{-3}–10^{-5} W/m^2). Their spectra SX are plotted on the logarithmic scale.

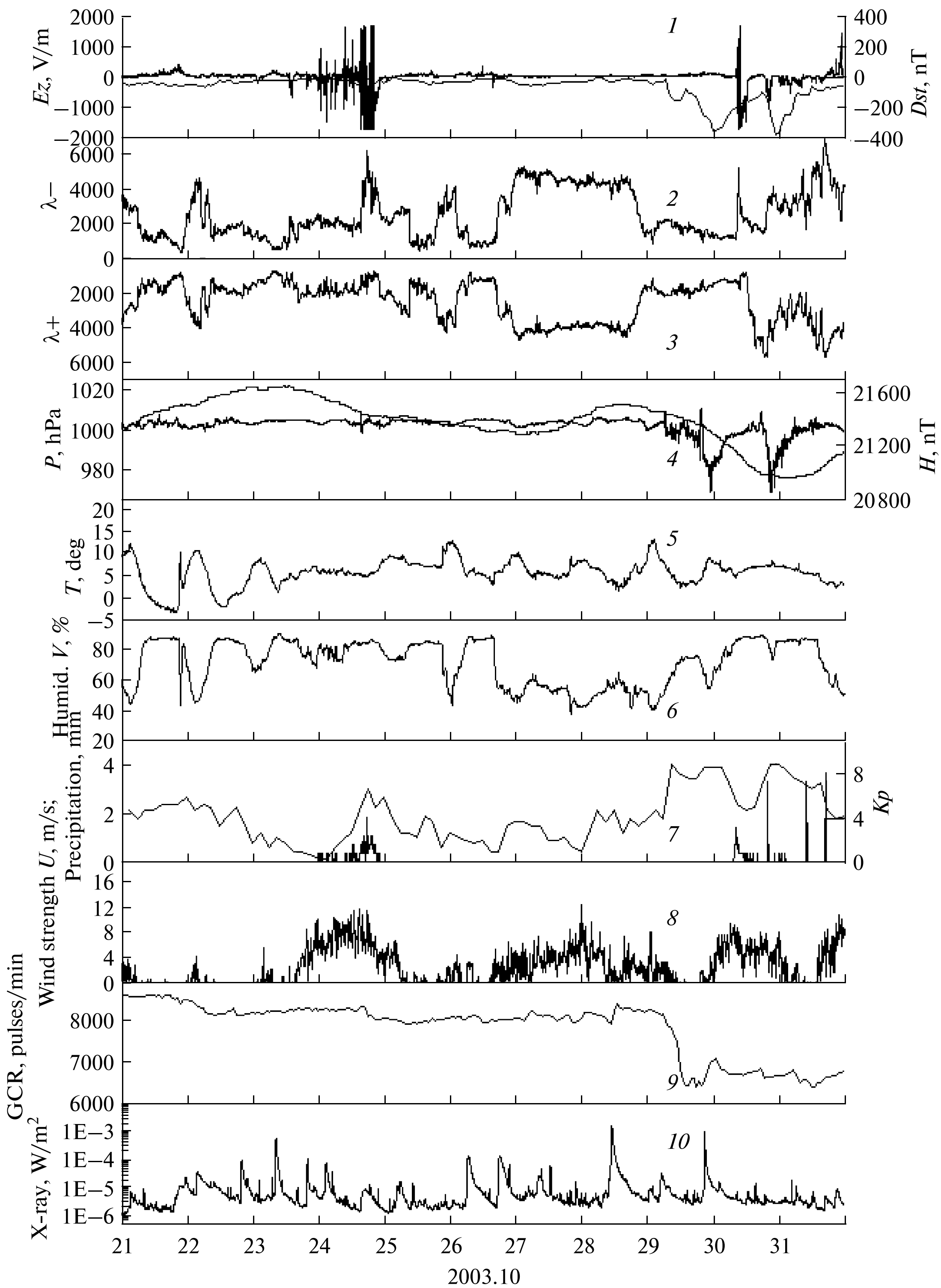

Fig. 1. Diurnal variations in the electric field, electric conductivity of the atmosphere, meteorological, geophysical and solar variables in October 21–31, 2003.

4. MAIN RESULTS AND DISCUSSION

Figure 3 shows the power spectra of the variables given in Fig. 1 for selected time intervals: October 21–22 (days of good weather); October 22–23 (a period of high solar activity with a series of solar flares (X rays up to 10^{-4} W/m^2)); October 24–25 (a period of high ($Kp \sim 6$) geomagnetic activity with emerging strong thunderstorm activity); October 28–29 (a complex

Flare events in AO 10484 and 10486 during October 19–31, 2003 and their manifestations in near-Earth space [Veselovskii et al., 2004]; the *Dst* and *kp* data were taken from http://spidr.ngdc.noaa.gov/spidr/ and http://wdc.kugi.kyoto-u.ac.jp/cgi-bin/kp-cgi, respectively

Date	Flare		*SC* UT	*Dst*, nT	*Kp*	Solar cosmic rays *E*, MeV *P*, $cm^{-2} s^{-1} sr^{-1}$	ГКЛ, %@	Main phase of storm
	Time UT Duration, min	Class						
19	16:29; 79	X1.1/1N		–40	5–			
22	19:45; >41	M9.9		–33	3–			
23	08:17; 64	X5.4/1B		–21	2		–5	
23	19:50; 38	X1.1/1N		–11	1–		–5	
24	02:22; 66	M7.6/1N		–8	1+		–3	
26	05:17; 213	X1.2/3B		–27	2		–7	
26	17:17; 179	X1.2/1N		–5	3–	2; 10	"	
26	21:26; 60	M7.6/2N		–16	4–		"	
27	09:21; 23	M5.0/1F		–49	2		–6	
27	12:27; 37	M6.7/1F		–41	2		"	
28	09:51; >269	X17.2/4B		–30 –80	4+ 8–	1 1000	–10	
29	20:37; 136	X10.0/2B		–233	9–	"	–5 –25	14.00–29
30				–350	9–	"	–15	00.01 30 τ = 11 h
30				–100	9	"	–22	18.00–30
30				–383	9	"	–24	23.00 30 τ = 5 h

period with two solar flares and simultaneously high geomagnetic activity ($Kp \sim 9$)); October 29–30 (a single but sufficiently powerful ($\sim 10^{-3}$ W/m^2) solar flare with a prolonged period of high geomagnetic activity and a Forbush decrease in galactic cosmic rays); October 30–31 (a period of high geomagnetic activity with short-term thunderstorm activity).

Figures 3a and 3b make it possible to trace the variations in the power spectra of given parameters from October 21 to 31 (vertical sections) and the relationship between these parameters in some time periods (horizontal sections).

We consider variations in the power spectra of the meteorological variables: air temperature and humidity (*ST* and *SV*).

Under the good weather conditions of October 21–22, before the strong solar flare, thermal radiation with known diurnal variations goes to the ground through the so-called window of transparency (infrared and visible light as well as far UV-radiation) and controls the power spectrum of temperature and humidity. As a result, their spectra (*ST* and *SV*) have the components of thermal tidal waves: S_{max} at $T \cong 24$ h and weak additional maxima at $T \sim 12$ and 48 h.

With increased solar activity on October 22–23, the temperature spectrum *ST* has an emerging component unresolved by frequency and with $T \sim 48$ h, which later (during the magnetic storm of October 24–25) becomes predominant, and the intensity of components with $T \sim 12$ and 24 h significantly decreases. Then, with the development of solar and geomagnetic activity, both components with $T \sim 24$ and 48 h can be amplified or weakened but are constantly present in the spectrum *ST*. The same complex changes are experienced by the power spectra of air humidity (*SV*). Their character is additionally modified by precipita-

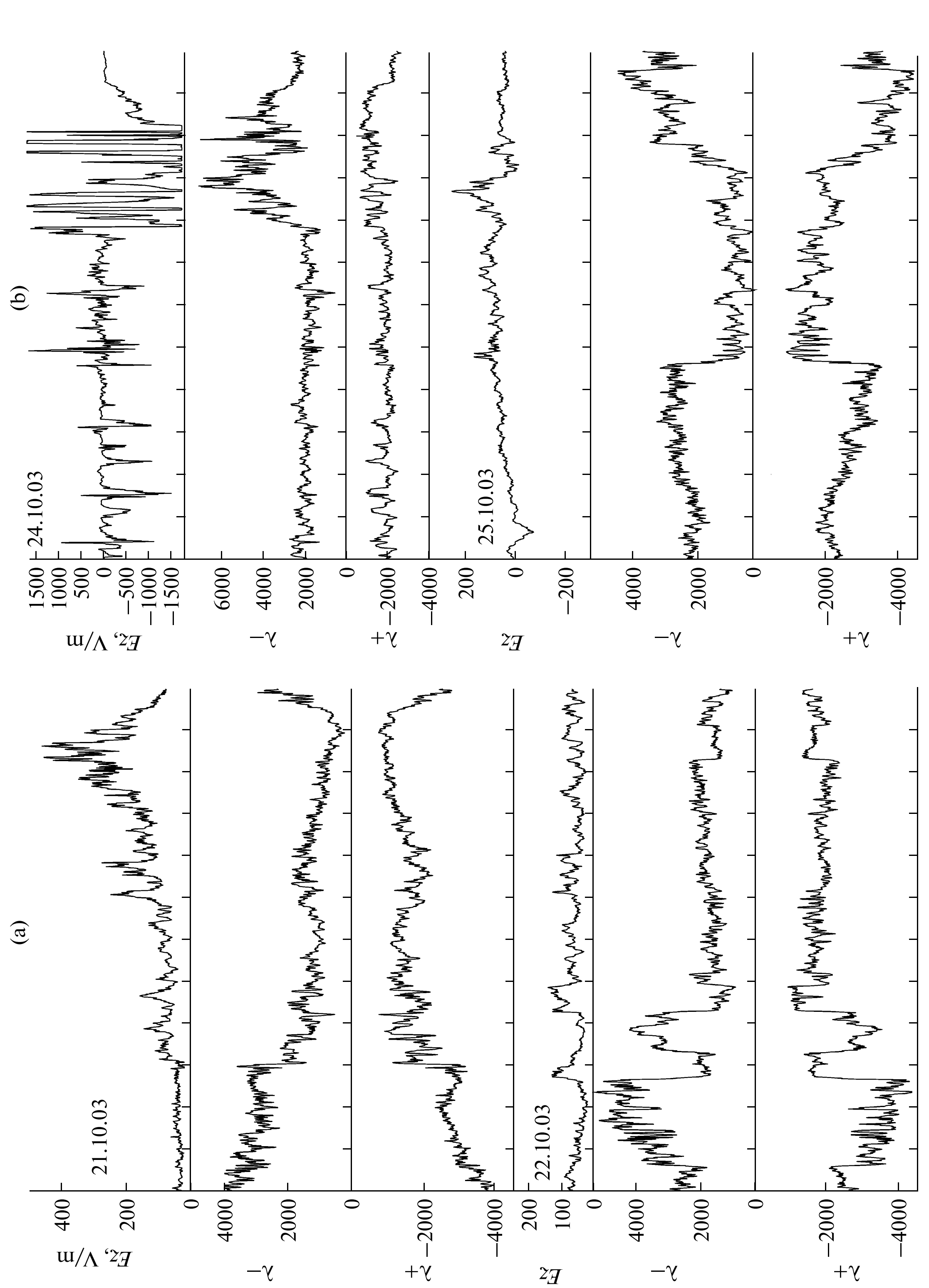

Fig. 2. Diurnal variations in the electric field stress and electric conductivity of the atmosphere in selected observation intervals (a, b, c, d).

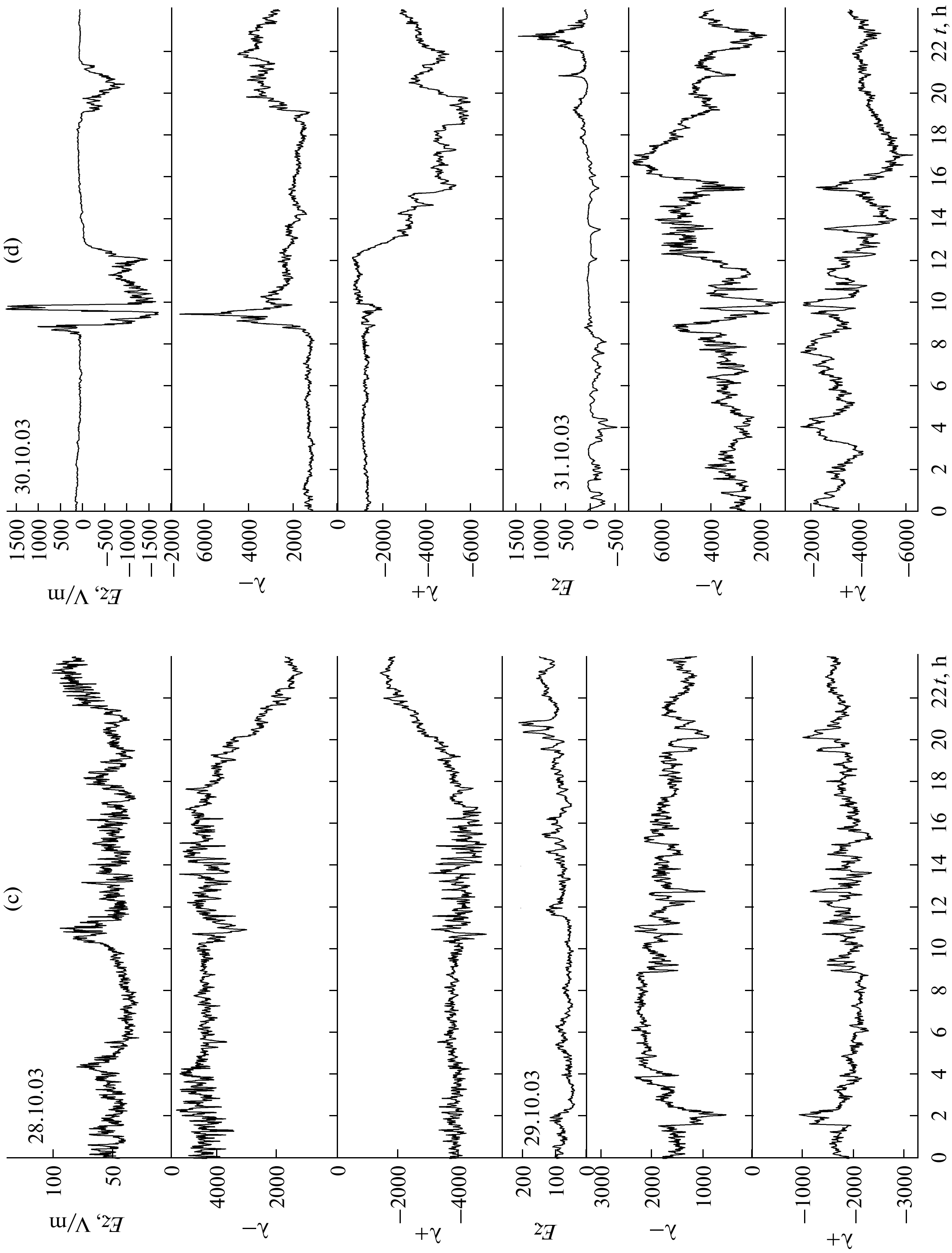

Fig. 2. (Contd.).

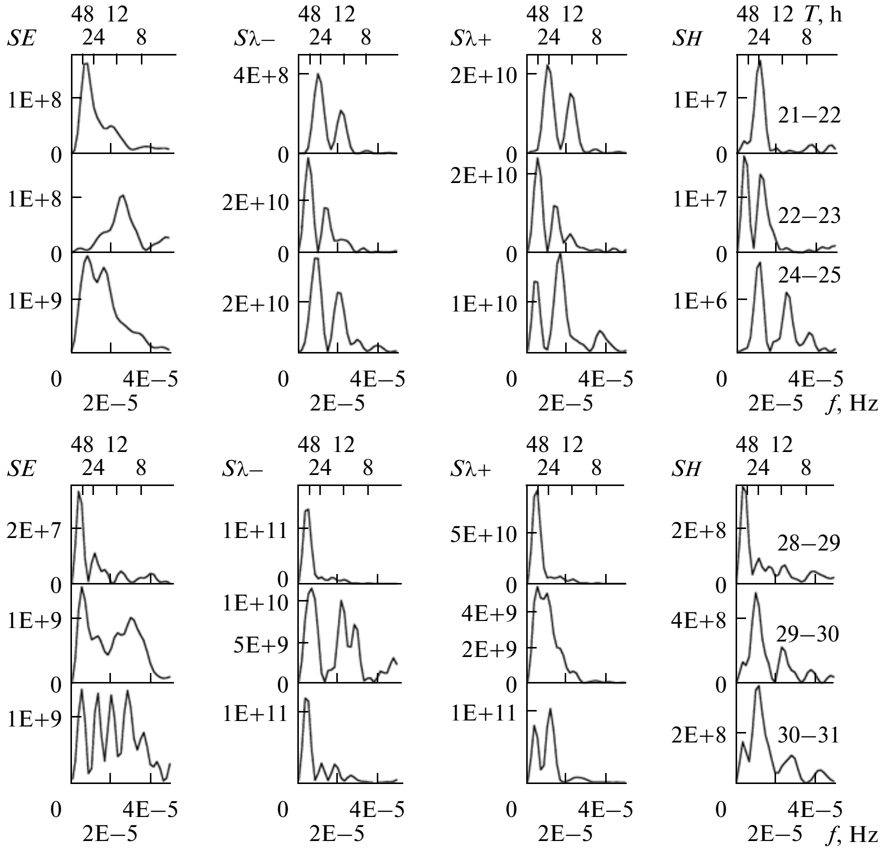

October 2003; $dt = 10$ min

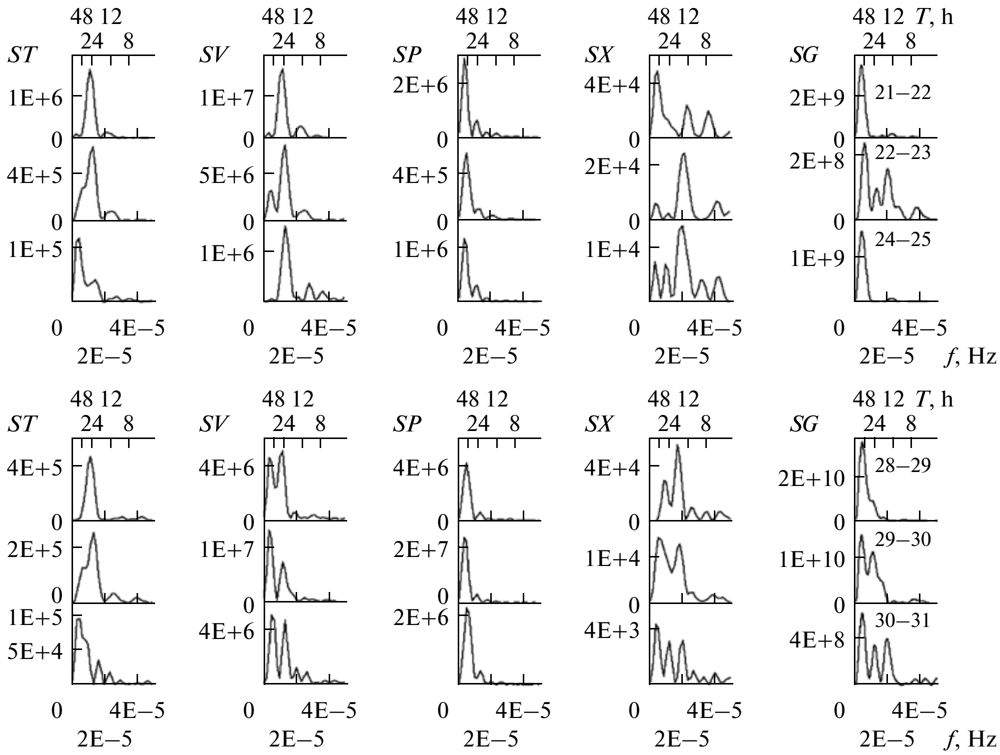

October 2003; $dt = 10$ min (for SG $dt = 1$ h)

Fig. 3. Series of curves of spectral density of the power of parameters given in Fig. 1 for the events specified in Fig. 2. The lower axis of abscissa indicates the frequency f (Hz) and the upper axis indicates the respective periods T.

tion during thunderstorm processes on October 24, 30, and 31. The character of the spectra is completely different in the variations of air pressure (*SP*) throughout the development of solar and geomagnetic processes: there is a predominant component with $T \sim 48$ h with weakly expressed component at $T \sim 24$ h. Here, the intensity of this peak varies slightly, except the period of October 29–30, when there is an increase in the spectral density of almost an order of magnitude.

Next, we consider the power spectra of the X-ray radiation of the sun (*SX*) and galactic cosmic rays (*SG*).

It is known [Fontenla et al., 2004; Woods et al., 2004] that the presence of an active area on the solar disc increases the radiation flux in the entire range of electromagnetic radiation. To estimate the wave processes on the sun, we use data on X-ray radiation intensity characterizing the intensity of flares. In our case, this is a rather rough approach to the estimation of processes in the near-surface atmosphere). The analysis of *SX* spectra shows the following: under good weather conditions of October 21–22, the *SX* spectrum involves a wide range of components and thermal tidal waves (24, 12, 8 h) and planetary-scale waves ($T \sim$ 48 h). With the development of solar and geomagnetic activities, the spectral composition is preserved but the intensity of various components varies greatly. It can be assumed that a similar character of the spectrum is preserved also in the band of atmospheric transparency window, through which the ground receives additional heat influx affecting the air temperature and humidity.

This time period was characterized by equally complex power spectra of galactic cosmic rays (*SG*). Under the good weather conditions of October 21–22, temporal variation in galactic cosmic rays (Fig. 1, curve *10*) involves a relatively weak decrease in the flux of galactic cosmic rays, which was caused by the earlier solar flare of October 20 (not shown in the figure but can be found in [Yermolaev et al., 2004]). The next decrease in the flux of galactic cosmic rays accompanied the October 23 flare, which also is reflected in the spectrum by the increased component with $T \sim 48$ h. When the flux significantly decreases on October 29, the intensity of this component grows by an order of magnitude in comparison to the period of October 21–22. In the recovery period, the power spectra *SG* are characterized by the fact that the dominant component with $T \sim 48$ h was coupled with components with $T \sim 12$, 24 h. Since the reduction in the intensity of fluxes of galactic cosmic rays is caused by increased solar wind blocking these fluxes, it can be assumed that the spectral composition of galactic cosmic rays is determined by the periodicity of solar processes, which also is reflected in the spectral composition of X rays.

Let us consider the power spectra of atmospheric electricity parameters: electric conductivity of air $S\lambda_+$ and $S\lambda_-$ and the electric field stress *SE*. Under the good weather conditions of October 21–22, the power spectrum *SE* is dominated by a broad maximum of intensity in the band of periods 24 h < T < 48 h and a weaker maximum with $T \sim 12$ h. Under the solar activity of October 22 and 23, the spectrum changed so that almost all of the power proved to be concentrated in the band of periods 12–24 h. At the same time, during the solar flares on October 28–29, the power spectrum was enriched by a component in a wide range of periods 12–48 h. During the magnetic storms on October 24–25 and 29–30, the spectrum was dominated by the components with $T \sim 48$ h, the intensity of which is an order of magnitude higher than that of the corresponding component on October 21–22. The complex character of the spectrum *SE* on October 24–25 and October 30–31 is associated with the influence of thunderstorm activity observed in these days.

The power spectra $S\lambda_+$ and $S\lambda_-$ had an equally complex character in these days. Under the good weather conditions of October 21–22, the spectrum has two components with 12 and 24 h, coinciding with the periods of thermal tidal waves. However, with increased solar activity on October 22–23, the dominant component with $T \sim 48$ h increased on the background of components with $T \sim 24$, 12, 8 h. During a magnetic storm and due to correspondingly reduced fluxes of galactic cosmic rays, the power spectra $S\lambda_+$ and $S\lambda_-$ expanded to the range of higher periods ($T \sim$ 48 h). The appearance of thunderstorm processes accompanied by precipitation carrying additional volumetric charges leads to components with $T \sim 12$ h that have a weaker intensity than the component with $T \sim 48$ h.

Within the model of a spherical capacitor, the current density in the atmosphere is determined by the following expression [Tverskoi, 1949]

$$j = \lambda E + \rho v + D_t \Delta\rho + \Sigma j_s,$$

where $\lambda = e\Sigma(n_{i+}U_{i+} + n_{i-}U_{i-})$, n_i is the concentration of positive and negative ions prevailing in the lower atmosphere, λE is the conduction current controlled by the thunderstorm generator, ρ is the volumetric charge, v is the medium motion velocity, and D_t is the eddy diffusivity. The last term of the expression describes currents of different sources, including precipitation currents ($j = \Sigma q_m n_m v_m$, where q_m is the charge, n_m is the concentration, and v_m is the rate of particle deposition during precipitation) and currents of global sources (solar cosmic rays and galactic cosmic rays), contributing to the current of the global electric circuit.

Under good weather conditions, the effect of solar activity on current density j and, accordingly, on the electric field stress is manifested in several ways. First, this occurs through variation in air conductivity, which is determined by the concentration and mobility of ions. As a result of low temperatures in October (curve *5*, Fig. 1) and the presence of snow cover and precipitation (curve *7*, Fig. 1), the release of subsurface air containing radon was delayed [Moses et al., 1960]. Since the contribution of galactic cosmic rays to the lower troposphere is insignificant, the air conductivity under slightly varying concentration of ions is determined by their mobility, which depends on the air temperature [Brikar, 1969]. In addition, the coupling with solar activity is reflected in the effects of sunrise and sunset through the local convective generator [Smirnov, 2013], when the temperature growth leads to an increase in the convective and turbulent heat fluxes contributing to the current density (the terms ρv and $D_t\nabla\rho$). This coupling with solar activity was reflected in the coinciding variations in the power spectra of temperature (*ST*), humidity (*SV*), electric conductivities ($S_{\lambda\pm}$), and, partly, *SE*, which involve the components of thermal tidal waves. Additionally, the influence of solar activity appeared through the action of clouds and precipitation, which were observed at the Paratunka observatory during the given period sporadically rather than periodically. Their contribution was manifested in variations in electric conductivity (curves *2* and *3*, Fig. 1).

Under disturbed conditions with strong solar flares (see the table), the GEC is characterized by the activation of global atmospheric ionizers: solar and galactic cosmic rays. As seen in Fig. 22 in [Veselovskii et al., 2004], during the period of October 21 to 31, after the strong solar flare on October 26, the flux of nuclei of solar cosmic rays in the northern hemisphere increased from 1 to $\sim 10^2$ on October 27 and to $\sim 10^3$ h/cm^2 s sr on October 28–29 under relatively quiet variations in galactic cosmic rays (curve *9*, Fig. 1). It is known that this reduces the threshold of strong cut-off of fluxes of solar cosmic rays. This leads to an increase in the concentration of tropospheric ions and, accordingly, the conductivity in the GEC. Apparently, this process can qualitatively explain the high constant level of electric conductivity on October 27 and 28 and the presence of the dominating component with $T \sim 48$ h in the spectra $S(\lambda_{+\,-})$ and *SE*. However, the start of the geomagnetic storm and the strong effect of the Forbush decrease of galactic cosmic rays at 16:00 UT (curve *10*, Fig. 1) suppressed the action of solar cosmic rays and extended the power spectra $S\lambda_{\pm}$ and *SE* to shorter periods ($T < 48$ h). As a result, the global sources of atmospheric ionization in this anomalous period of solar activity suppressed the action of local sources: convective generator, clouds, and precipitation.

5. CONCLUSIONS

Studies of the power spectra of meteorological and electrical variables in the near-surface atmosphere in Kamchatka during solar events in October 2003 revealed the following:

(1) Under good weather conditions, the power spectra of atmospheric temperature and humidity had oscillations with periods of thermal tidal atmospheric waves ($T \sim 12$, 24 h) caused by the of solar heat influx.

(2) During strong solar flares accompanied by additional heat influx entering into the lower troposphere, the diurnal variation and feedback between temperature and humidity are disturbed. When the component with $T \sim 24$ h is dominating, the humidity spectrum has an additional component with $T \sim 48$ h (the period of planetary-scale atmospheric waves).

(3) This power spectrum of these variables is retains during the magnetic storm on October 29–31.

(4) Under good weather conditions, the power spectra of atmospheric pressure is characterized by a wide range of oscillations 12, 24, 48 h, with $T \sim 48$ h being the dominant component. With the development of solar activity, the spectrum retained its character; however, the intensity of the component with $T \sim 48$ h during the geomagnetic storm increased by an order of magnitude in comparison with good weather conditions.

(5) Under good weather conditions, the power spectra of electric conductivity of the atmosphere involve components with $T \sim 12$ and 24 h. At the same time, the power spectrum of the electric field is characterized by the fact that these components are weakly expressed and the component $T \sim 48$ h is predominant.

(6) During strong solar flares and magnetic storms, the power spectra of electric conductivity components had clearly expressed components nearly with the same intensity as at $T \sim 24$ and 48 h. The electric field spectrum was more complex (due to the influence of thunderstorm processes) but with a predominant component $T \sim 48$ h, the intensity of which increased by an order of magnitude in comparison with good weather conditions. This character of the power spectrum of the electric field was also observed during solar and geomagnetic events in November 2004 [Smirnov et al., 2013].

(7) In the power spectra of galactic cosmic rays accompanying strong solar flares, the component with $T \sim 48$ h was predominant and increased by an order of magnitude during the Forbush decrease on October 29. This character of spectra was also observed during the magnetic storms in November 2004 [Smirnov et al., 2013]. The simultaneous amplification of components with $T \sim 48$ h in the power spectra of electric conductivity of air and electric field stress points to the fact that during strong solar flares and magnetic storms, the role of the actual ionizer of the lower troposphere is mainly played by galactic cosmic rays.

(8) The specified oscillation period with $T \sim 48$ h in the spectra of galactic cosmic rays and of X-ray radiation of the sun seems to be caused by the dynamics of solar and geomagnetic activities with this time scale.

ACKNOWLEDGMENTS

The authors are grateful to V.K. Mikhailov for assistance in the preparation of this manuscript.

REFERENCES

Bricard, J., Action of radioactivity and pollution upon parameters of atmospheric electricity, *Problems of*
1 *Atmospheric and Space Electricity*, Coronity, C.C., Ed., Amsterdam: Elsevier, 1965, pp. 82–117.

Fontenla, J.M., Harder, J., Rottman, G., et al., The signature of solar activity in the infrared spectral irradiance, *Astron. J.*, 2004, vol. 605, pp. L85–L88.

Lebedinskii, A.I., Andrianov, Yu.G., Karavaev, I.I., et al., Correlations of the dependence of spectral intensity of the Earth's infrared radiation in the space, *Geomagn. Aeron.*, 1968, vol. 8, no. 1, pp. 9–14.

Moses, H., Stehnly, A.F., and Lucas, H.F., The effect of meteorological variables upon the vertical and temporal distributions of atmospheric radon, *J. Geophys. Res.*, 1960, vol. 65, no. 4, pp. 1223–1238.

Roble, R.G., On solar–terrestrial relationships in atmospheric electricity, *J. Geophys. Res.*, 1985, vol. 90, no. D4, pp. 6000–6012.

Rycroft, M.J., Nicoll, K.A., Alpin, K.L., and Harrison, R.G., Recent advances in global electric circuit coupling between the space environment and the troposphere, *J. Atmos. Sol.–Terr. Phys.*, 2012, vol. 90–91, pp. 198–211. http://dx.doi.org/10.1016/j.jastp.2012.03.015.

Smirnov, S.E., Mikhailova, G.A., and Kapustina, O.V., Variations in the quasi-static electric field in the near-Earth's atmosphere during geomagnetic storms in November 2004, *Geomagn. Aeron.*, 2013, vol. 53, no. 4, pp. 502–514. doi 10.1134/S0016793213040130

Smirnov, S.E., Influence of a convective generator on the diurnal behavior of the electric field strength in the near-Earth atmosphere in Kamchatka, *Geomagn. Aeron.*, 2013, vol. 53, no. 4, pp. 515–521. doi 10.1134/S0016793213040142

Smirnov, S.E., Mikhailova, G.A., and Kapustina, O.V., Variations in electric and meteorological parameters in the near-Earth's atmosphere at Kamchatka during the solar events in October 2003, *Geomagn. Aeron.*, 2014, vol. 54, no. 2, pp. 240–247. doi 10.1134/S0016793214020182

Tverskoi, P.N., *Atmosfernoe elektrichestvo* (Atmospheric Electricity), Leningrad: Gidrometeoizdat, 1949.

Veselovsky, I.S., Panasyuk, M.I., Avdyushin, S.I., et al., Solar and heliospheric phenomena in October–November 2003: Causes and effects, *Cosmic Res.*, 2004, vol. 42, no. 5, pp. 435–488.

Woods, T.N., Eparvier, F.G., Fontenla, J., et al., Solar irradiance variability during the October 2003 solar storm period, *Geophys. Res. Lett.*, 2004, vol. 31, L10802. doi 10.1029/2004GL019571.

Translated by V. Arutyunyan

SPELL: 1. OK